FINITE ELEMENT MODELING OF ATHEROSCLEROTIC PLAQUE BASED ON OPTICAL COHERENCE TOMOGRAPHY

Alexandra H. Chau (1,3), Mohammad R. Kaazempur-Mofrad (1,2,7), Raymond C. Chan (6), Guillermo J. Tearney (3,4,5), Brett E. Bouma (3,4), Roger D. Kamm (1,2)

(1) Department of Mechanical Engineering
(2) Division of Biological Engineering
Massachusetts Institute of Technology
Cambridge, MA

(3) Wellman Laboratories of Photomedicine,
(4) Dermatology, (5) Pathology, (6) Radiology, (7) Surgery
Harvard Medical School & Massachusetts General Hospital
Boston, MA

ABSTRACT

Intravascular optical coherence tomography (OCT) provides high-resolution images for finite element modeling of detailed stress distributions within atherosclerotic plaques. Due to limited depth penetration, however, outer plaque boundaries can be ambiguous in OCT. This study demonstrates the first use of OCT for image-based finite element modeling and investigates the sensitivity of estimated stress patterns to variations in the outer boundary location. The results indicate that OCT-based FEM models are as detailed as those from histology and that outer boundary ambiguity has minimal effect on intra-plaque stress distributions, validating the use of OCT as a basis for finite element modeling.

INTRODUCTION

Rupture of vulnerable atherosclerotic plaques can result in myocardial infarctions or strokes, the leading causes of death and disability in the U.S. Finite element analysis can identify areas of stress concentration prone to rupture and can thus be used to assess lesion stability. Accurate finite element analysis requires detailed knowledge of plaque geometry derived from either imaging or histology, the current gold standard. This study investigates the use of a recently developed intravascular imaging modality based on optical coherence tomography (OCT) for generating image-based finite element models.

METHODS

OCT Imaging

Intravascular OCT scanning is performed with a custom-built system. OCT catheters are constructed from modified 3.2 F IVUS catheters (Boston Scientific, Natick, MA). The in-plane resolution of this OCT system is 10 µm. OCT images of *ex vivo* coronary cross-sections were acquired with a motorized catheter pullback of 0.5mm/s and a frame rate of 4 Hz (500 angular pixels x 250 radial pixels). This modality allows identification of individual plaque components, including thin fibrous caps, the detection of which is not possible with other imaging modalities [1]. Figure 1A-B shows an OCT image of a lipid rich plaque, with the corresponding histology section.

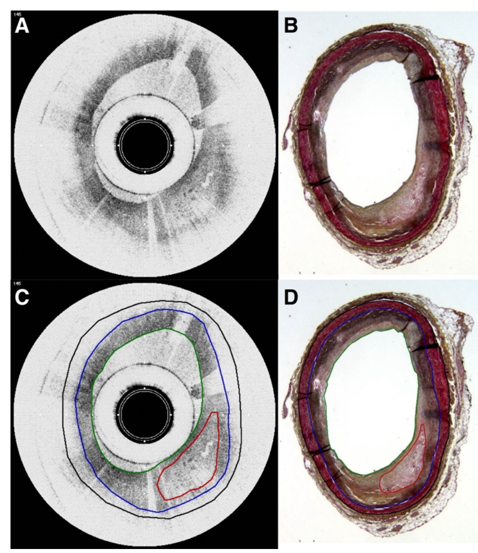

Figure 1. A. OCT image of a coronary lipid-rich plaque cross section, and B. the corresponding histology section. C. segmented OCT image of a lipid rich plaque, and D. the corresponding segmented histology section. The inner lumen boundary is shown in green, the lipid-rich region is outlined in red, the fibrous plaque is shown in blue, and the outer arterial wall boundary is black.

Segmentation

OCT images were segmented by an expert pathologist to identify the boundaries of normal, lipid-rich, calcific, and fibrous tissue regions. In Figure 1C-D, a segmented OCT image is shown with its corresponding segmented histology section. This example demonstrates two major points. First, the ability of OCT imaging to produce high-resolution structural and compositional data that are comparable to histology, yet are uncorrupted by the artifacts that accompany histological processing. Second, the difficulty of localizing the outer plaque boundaries in OCT due to its limited depth of penetration.

Finite element modeling

A commercial FEM package, ADINA (Watertown, MA), was used to create and run the models. The segmented boundary data shown in Figure 1 were used as geometry lines for finite element modeling. Each region was modeled as a rubber-like material, defined with Mooney-Rivlin parameters D_1 and D_2, the coefficients of the strain energy density function. An example FEM mesh for the lipid rich plaque is shown in Figure 3. The red area is lipid (D_1=50.0 Pa, D_2=5.0), the green region is fibrous plaque (D_1=5105.3.0 Pa, D_2=13.0), and the blue mesh is normal arterial wall (D_1=2644.7 Pa, D_2=8.365) [2-4]. A pressure load, ramping from 0 to 16 kPa over 32 time steps, was applied at the vessel lumen to obtain the stress distribution under physiological conditions.

To determine the effect of ambiguous segmentation at the outer plaque boundary, the border location was systematically varied while the outer arterial wall boundary remained constant. The finite element models were modified to reflect these new plaque boundaries, with the material properties, boundary conditions, and loading remaining the same. The effect on the estimated stress patterns from finite element modeling was then examined. Figure 2 illustrates three candidate locations for the outer plaque boundary: the original outer boundary, a shrunken boundary (area reduction of 24%), and an expanded boundary (area increase of 32%). These values were chosen to represent a reasonable range of segmentation errors.

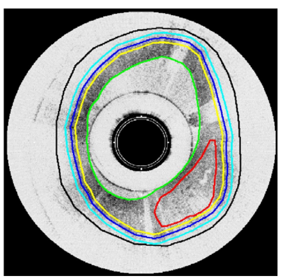

Figure 2. The segmented OCT image overlaid with three outer plaque boundaries: the original plaque boundary (in dark blue), a boundary shrunken by 80 μm (in yellow), and a boundary expanded by 100 μm (in light blue) are shown.

RESULTS

The effective stresses for each of the three models are shown in Figures 3-4. As expected, the lipid pool exhibits the lowest levels of stress, while the fibrous cap separating the lipid pool from the lumen experiences elevated stresses, to compensate for low lipid stiffness and inability of lipids to support load (see Figure 3) [3]. High curvature features are responsible for other stress concentrations observed in the fibrous plaque. Variation of the border location did not generally affect the stress distribution (see Figure 4). Increasing the plaque area by 32% reduces the overall stress magnitude in the plaque (Figure 4A), whereas decreasing it by 24% yields increased stress magnitudes (Figure 4B). This result is consistent with the material properties chosen – fibrous plaque is the stiffest material and is therefore expected to carry the most stress. When plaque thickness is increased, the load is distributed throughout a greater thickness, reducing overall stress magnitudes.

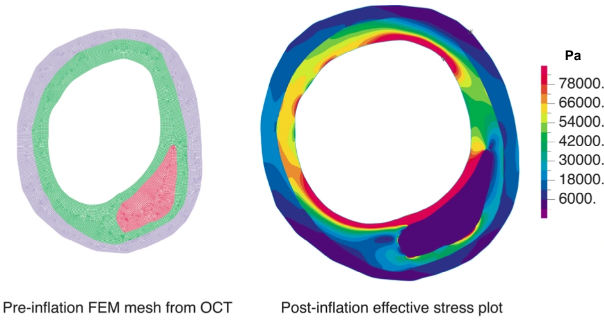

Figure 3. OCT-derived FEM mesh for the lipid rich plaque (left) with corresponding effective stress [pa] plot (right).

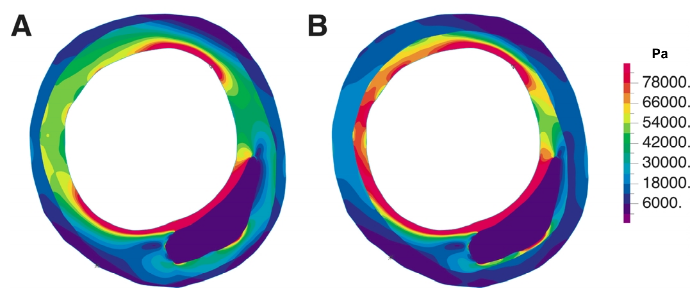

Figure 4. Effective stress [Pa] plots for A. the expanded plaque boundary, and B. the shrunken plaque boundary

CONCLUSION

We presented the first use of OCT for image-based finite element modeling and have investigated the sensitivity of stress patterns to variations in the plaque outer boundary. Our results demonstrate that OCT-based FEM models are nearly as detailed as those from histology and that outer plaque boundary uncertainty exerts minimal influence on intra-plaque stress distributions. Models based on varying plaque thickness exhibit similar stress distribution, suggesting that segmentation ambiguities at the outer wall do not significantly degrade the quality of finite element analysis results. Work in progress suggests that this is also the case for segmentation ambiguities in the outer arterial wall boundary. OCT-based FEM is potentially superior to modeling based on other imaging modalities since OCT allows for *in vivo* imaging of *intact* specimens with spatial resolution approaching that of histology.

REFERENCES

1. Yabushita, H., and Bouma, B. E., 2002, “Characterization of Human Atherosclerosis by Optical Coherence Tomography,” *Circulation*, Vol. 106, pp. 1640-1645.
2. Delfino, A. “Analysis of a stress field in a model of the human carotid bifurcation,” in Physics. Lausanne: Ecole Polytechnique Federale De Lausanne; 1996.
3. Loree, H.M., Tobias, B.J., Gibson, L.J., et al., “Mechanical Properties of model atherosclerotic lesion lipid pools,” in Arteriosclerosis Thromb. 1994; vol 14: pp.230-234.
4. Loree, H.M., Grodzinsky, A.J., Park, S.Y. et al. “Static circumferential modulus of human atherosclerotic tissue,” in J. Biomech. 1994; vol 27: pp.195-204.